Stabilization of Underactuated Systems of Degree One via Neural Interconnection and Damping Assignment Passivity Based Control

Sanchez Escalonilla Plaza, Santiago; Reyes-Báez, Rodolfo; Jayawardhana, Bayu

Published in:
61st IEEE Conference on Decision and Control

Publication date:
2022

Stabilization of Underactuated Systems of Degree One via Neural Interconnection and Damping Assignment – Passivity Based Control

Santiago Sánchez-Escalonilla, Rodolfo Reyes-Báez and Bayu Jayawardhana

***Abstract*— In this work, we show the *potential* of the universal approximation property of neural networks in the design of interconnection and damping assignment passivity-based controllers (IDA-PBC) for stabilizing nonlinear underactuated mechanical systems of degree *one*. Towards this end, we reformulate the IDA-PBC design methodology as a neural supervised learning problem that approximates the solution of the *partial differential* matching equations, which fulfills the equilibrium assignment and stability conditions. The output of the neural learning process has clear physical and control-theoretic interpretations in terms of energy, passivity and Lyapunov stability. The proposed approach is numerically evaluated in two well-known underactuated systems: the inverted pendulum on a cart and inertial wheel pendulum, whose analytic IDA-PBC solutions are non-trivial to obtain.**

I. INTRODUCTION

The IDA-PBC technique [1] is a popular nonlinear control design methodology for set-point regulation. It has been successfully applied to a variety of electromechanical systems, for which the target closed-loop dynamics takes the form of a port-Hamiltonian (pH) system with desired passivity and interconnection properties.

The technique comprises of two standard steps of passivity-based control (PBC) method, namely: (i) *energy-shaping* step that assigns the desired equilibrium x^* as the minimum of the shaped energy function; and (ii) *damping injection* step that ensures the dissipation of shaped energy function to achieve asymptotic stability. For the first step, one needs to solve a set of partial differential equations (PDEs), the so-called *matching equations* (ME), which is not trivial, in general. For mechanical systems, the aforementioned ME can be split into kinetic energy shaping ME and potential energy shaping ME [1]. The former one results in a *nonlinear* PDE whose solution is the target closed-loop inertia matrix; whereas the latter one corresponds to a linear PDE that defines the assignable potential energy functions. In the case of fully-actuated mechanical systems, these ME can trivially be solved, and typically only[1] the potential energy-shaping is involved. However, for underactuated systems, it is *necessary* to perform *total* energy-shaping [1] because the potential energy-shaping part can only be performed in the actuated degree-of-freedom. For the past decade, there are many works that investigate methods to construct explicit solutions of the ME for various classes of underactuated systems, such as, the works in [2], [3], [4], [5], [6], [7] among others. The construction of ME solutions in these papers typically relies on *mathematical assumptions* that are often very *restrictive* or *lack* of a clear physical interpretation.

In addition to the IDA-PBC approach, finding closed-form solutions to some PDEs has also been a central problem in many other control design methods, such as, the nonlinear output regulation problem [8] or the immersion & invariance method [9], which are non-trivial. In this context, recent advances in machine learning [10] are enabling the possibility of constructing parametric models that are interpretable from a first-principle point of view and therefore can be used as surrogates in model-based control design approaches. The benefit of using these parametric models is that it allows control designers to use existing model-based control methods without losing insights and properties of the closed-loop systems. In recent years, their applicability in analysis and design of control systems has been studied in [11], [12], [13], [14], [15], [16].

In our previous work [17], we presented a method to solve the aforementioned ME of IDA-PBC in fully actuated systems by transforming it into a neural supervised learning problem, which is motivated by the *universal approximation* property of neural networks (NNs) [18]. On one hand, as briefly mentioned before, solving such ME problem for fully actuated systems can be achieved simply by potential energy shaping that leads to simple (constant) forms of the assigned interconnection and damping matrices [17, Section 4]. On the other hand, solving ME problem for underactuated systems also *requires* the kinetic energy shaping part [1], which generates an extra set of ME that introduce complication in finding the right *ansatz* solutions. Correspondingly, in this paper, we present an extension of our previous work that can freely explore these non-trivial assigned interconnection and damping matrices. This approach results in a control-informed NN design method for IDA-PBC, and is referred to as *Neural IDA-PBC*.

The rest of this paper is structured as follows. Section II provides the preliminaries necessary for the context of this paper. In Section III we systematically construct a cost function to embed the IDA-PBC design methodology and pH systems' first principles. In Section IV the proposed methodology is validated with the simulation of two underactuated systems. Finally, Section V contains some concluding remarks.

This publication is part of the project Digital Twin project 6 with project number P18-03 of the research programme Perspectief which is (mainly) financed by the Dutch Research Council (NWO).

S. Sánchez-Escalonilla, R. Reyes-Báez and B. Jayawardhana are with the Jan C. Willems Center for Systems and Control, Engineering and Technology Institute Groningen (ENTEG), University of Groningen, The Netherlands {santiago.sanchez, r.reyes-baez, b.jayawardhana}@rug.nl

[1]Even in the fully-actuated case, total energy-shaping can be beneficial to meet some closed-loop performance metrics.

II. PRELIMINARIES

A. Underactuated mechanical port-Hamiltonian systems

Using the port-Hamiltonian framework (see, for example, [19]), the dynamics of standard mechanical systems with generalized coordinates q on the configuration space $\mathcal{Q} \subset \mathbb{R}^n$ and velocity $\dot{q} \in T_q\mathcal{Q}$ can be given by

$$\dot{x} = [J(x) - R(x)]\frac{\partial H}{\partial x}(x) + g(x)u, \quad y = g^\top(x)\frac{\partial H}{\partial x}(x), \quad (1)$$

with the Hamiltonian given by the total energy of the system

$$H(x) = \frac{1}{2}p^\top M^{-1}(q)p + U(q), \quad (2)$$

where $x = (q, p) \in \mathcal{X}$ is the state and $p := M(q)\dot{q}$ is the generalized momentum. The scalar function $U(q)$ is the potential energy, and $M(q) = M^\top(q) > 0$ is the inertia matrix. The interconnection, dissipation and input matrices are, respectively, given by $J = \begin{bmatrix} 0_n & I_n \\ -I_n & 0_n \end{bmatrix}$, $R = \begin{bmatrix} 0_n & 0_n \\ 0_n & D(x) \end{bmatrix}$, $g = \begin{bmatrix} 0_n \\ B(q) \end{bmatrix}$, where the $n \times n$ matrix $D(x) = D^\top(x) \geq 0_n$ is a dissipation term, and I_n and 0_n are the $n \times n$ identity and zero matrices, respectively. The input u represents generalized forces while the output y gives the generalized velocity so that their inner-product describes power. As we are interested in underactuated systems, the input force matrix $B(q)$ is assumed to have the rank $m < n$. The rate of change of $H(x)$ provides a power balance relation between the internal power of system (1) and the external supplied power:

$$\dot{H}(x) = -\frac{\partial H^\top}{\partial p}(x)D(x)\frac{\partial H}{\partial p}(x) + y^\top u \leq y^\top u, \quad (3)$$

where the inner-product $y^\top u$ is the external supplied power. In the context of *dissipativity theory*, the inequality (3) shows that the map $u \mapsto y$ is *passive* with respect to the storage function $H(x)$ in (2) and the supply rate $y^\top u$. We refer interested reader to [20, Section 6.2].

B. IDA-PBC design methodology

The IDA-PBC technique, as proposed in [1], is a control design method whose main control objective is to design a *static* state feedback control law of the form $u(x) = \beta(x) + v$ for the pH system in (1), such that the closed-loop dynamics are given by

$$\dot{x} = [J_d(x) - R_d(x)]\frac{\partial H_d}{\partial x}(x) + g(x)v, \quad y' = g(x)^\top\frac{\partial H_d}{\partial x}(x), \quad (4)$$

where $H_d(x)$, $J_d(x) = -J_d^\top(x)$ and $R_d(x) = R_d^\top(x) \geq 0$ are the *desired* Hamiltonian, interconnection and damping matrices, respectively. The desired Hamiltonian $H_d(x)$ has a strict local minimum at the desired equilibrium point $x^\star = (q^\star, 0)$ and the pair (v, y') is the new power conjugate pair that defines the desired passivity relation with storage function $H_d(x)$.

*Theorem 2.1 (*IDA-PBC [1]*):* Consider $J(x)$, $R(x)$, $H(x)$, $g(x)$ of the pH system in (1) and a desired equilibrium point $x^* \in \mathcal{X}$. Assume that there exist functions $J_d(x)$, $R_d(x)$ and $H_d(x)$ satisfying the *matching equation*

$$g^\perp(x)[J_d(x) - R_d(x)]\frac{\partial H_d}{\partial x} = g^\perp(x)[J(x) - R(x)]\frac{\partial H}{\partial x}, \quad (5)$$

where $g^\perp(x)$ is the full rank left annihilator of $g(x)$. Then system (1) in closed-loop with the control law

$$u = [g^\top g]^{-1}g^\top\left((J_d - R_d)\frac{\partial H_d}{\partial x} - (J - R)\frac{\partial H}{\partial x}\right), \quad (6)$$

takes the form (4) with $v = 0$, and x^* is locally stable. Moreover, x^* is asymptotically[2] stable if it is locally detectable from the output $y' = B^\top(x)\frac{\partial H_d}{\partial p}(x)$. The results holds globally if x^* is a global minimum of $H_d(x)$ and $H_d(x)$ radially unbounded.

After some straightforward algebraic manipulations, the desired functions can be rewritten as the sum of the functions $J(x), R(x), H(x)$ of the pH system in (1) and some *auxiliary* functions $J_a(x), R_a(x), H_a(x)$ such that

$$J_d := J(x) + J_a(x),\ R_d := R(x) + R_a(x)\ H_d := H(x) + H_a(x). \quad (7)$$

These auxiliary terms are used to *assign* the desired functions in the IDA-PBC methodology in Theorem 2.1. Some implicit design properties on these auxiliary functions are mentioned below as these are key for the constructive design procedure to be presented in Section III.

(P1) *Structure preservation*: the matrices $J_a(x)$ and $R_a(x) \geq 0$ are skew-symmetric and symmetric, respectively.

(P2) *Integrability*: $K(x) = \frac{\partial H_a}{\partial x}(x)$ is the gradient of a scalar function, i.e. $\frac{\partial K}{\partial x}(x) = \frac{\partial^\top K}{\partial x}(x)$.

(P3) *Equilibrium assignment*: $H_a(x)$ satisfies $\frac{\partial H_d}{\partial x}(x^\star) = \frac{\partial H}{\partial x}(x^\star) + \frac{\partial H_a}{\partial x}(x^\star) = 0$, where $x^\star = \mathrm{argmin}_{x\in\Omega}H_d(x)$.

(P4) *Lyapunov stability* $H_d(x)$ is a positive definite function at $x^\star$, i.e. $\frac{\partial^2 H_d}{\partial x^2}(x^\star) = \frac{\partial^2 H}{\partial x^2}(x^\star) + \frac{\partial^2 H_a}{\partial x^2}(x^\star) > 0$.

III. NEURAL IDA-PBC

A. NN approximated solutions of the matching equations

The main contribution of this work is based on the well-known universal approximation property of NN [18], [21]. In the following lemma, we propose an adaptation of the approximation theorem for the solution to the nonlinear output regulation control problem [11, Section 3] to the case of IDA-PBC technique (see Section II-B).

Lemma 1: Let $\{H_d(x), J_d(x), R_d(x)\}$ be a triplet satisfying the matching equations (5) and the conditions (P1)-(P4), and let $\mathcal{V}$ be a compact subset of $\mathcal{X}$. Then the triplet can be approximated by a sufficiently large (wide and deep) neural network to any prescribed precision on $\mathcal{V}$. That is, for any given $\varepsilon > 0$, there exist the triplet NN $\{\hat{H}_d(\theta; x), \hat{J}_d(\theta; x), \hat{R}_d(\theta; x)\}$ of the form (7), satisfying

$$\left\|\frac{\partial \hat{H}_d}{\partial x}(\theta; x) - \frac{\partial H_d}{\partial x}(x)\right\| < \varepsilon, \quad (8)$$

$$\left\|\hat{J}_d(\theta; x) - J_d(x)\right\| < \varepsilon, \quad (9)$$

$$\left\|\hat{R}_d(\theta; x) - R_d(x)\right\| < \varepsilon, \quad (10)$$

with θ be the vector of NN weights.

Due to space limitations, the proof of this lemma is omitted and it follows similar arguments as [11, Lemma 1].

[2] Equivalent conditions can be given in term of the LaSalle principle.

B. IDA-PBC-informed NNs

Based on Lemma 1, we present in this subsection the construction of NN that can approximate the design functions of the IDA-PBC design method. To that end, one can systematically construct a cost function that encodes the matching equations (5) and conditions (P1)-(P4). Once this cost function is minimized, the actual IDA-PBC design functions $(H_d(x), J_d(x), R_d(x))$ can be approximated by their corresponding NNs surrogates, respectively, as follows: $\hat{H}_d(\theta;x) := H(x) + \hat{H}_a(\theta;x)$, $\hat{J}_d(\theta;x) := J(x) + \hat{J}_a(\theta;x)$ and $\hat{R}_d(\theta;x) := R(x) + \hat{R}_a(\theta;x)$.

The aforementioned cost function is constructed as the sum of the following residuals defined on $\mathscr{V}$:

a) Equilibrium assignment: The approximated closed-loop energy function $\hat{H}_d(\theta;x) := H(x) + \hat{H}_a(\theta;x)$ has a local minimum at the desired equilibrium point $x^\star = (q^\star, 0)$:

$$f_{\text{eq}}(\theta;x^\star) := \|H_d(\theta;x^\star)\|^2 + \left\| \frac{\partial H_d}{\partial x}(\theta;x^\star) \right\|^2. \tag{11}$$

b) Lyapunov stability: The approximated closed-loop energy function must be convex. This is equivalent to having strictly positive elements in spectrum of $\frac{\partial^2 \hat{H}_d}{\partial x^2}(\theta;x)$. Additionally, $H_d(\theta;x) > 0$ for all x in the neighborhood of $x^\star$:

$$\begin{aligned} f_{\text{lyap}}(\theta;x) := \max\left\{0, a - \sigma\left(\frac{\partial^2 H_d}{\partial x^2}(\theta;x)\right)\right\} + \\ + \max\{0, b - H_d(\theta;x)\}. \end{aligned} \tag{12}$$

where σ denotes the spectrum of a matrix and $a, b > 0$ are constant values that can be added to make this condition stricter.

c) Matching equations: The approximated functions $(\hat{H}_a(\theta;x), \hat{J}_a(\theta;x), \hat{R}_a(\theta;x))$ must satisfy the ME in (5):

$$\begin{aligned} f_{\text{match}}(\theta;x) := \Bigg\| g^\perp(x)[\hat{J}_d(\theta;x) - \hat{R}_d(\theta;x)] \frac{\partial \hat{H}_d}{\partial x}(\theta;x) \\ - g^\perp(x)[J(x) - R(x)] \frac{\partial H}{\partial x}(x) \Bigg\|^2. \end{aligned} \tag{13}$$

d) Structure preservation: The approximated assigned damping matrix must be a symmetric and positive definite matrix $\hat{R}_a(\theta;q)$ of the form

$$\hat{R}_a(\theta;q) = \begin{bmatrix} 0_n & 0_n \\ 0_n & \hat{R}_{a^{(2)}}(\theta;q) \end{bmatrix}, \tag{14}$$

where $\hat{R}_{a^{(2)}}(\theta;q) := \operatorname{diag}\{\hat{R}_{a^{(2,1)}}(\theta;q), \ldots, \hat{R}_{a^{(2,n)}}(q)\} > 0$, In addition, the approximated of the assigned skew-symmetric interconnection matrix is defined as

$$\hat{J}_a(\theta;q) = \begin{bmatrix} 0_n & \hat{J}_{a^{(1)}}(\theta;q) \\ -\hat{J}^\top_{a^{(1)}}(\theta;q) & \hat{J}_{a^{(2)}}(\theta;q) \end{bmatrix}. \tag{15}$$

and the sub-block matrix $\hat{J}_{a^{(2)}}(\theta;q)$ is skew-symmetric.

As a consequence of the structural assumptions on $\hat{R}_a(\theta;q)$ and $\hat{J}_a(\theta;q)$, the last residual function is given by

$$\begin{aligned} f_{\text{struct}}(\theta;x) := \max\{0, cI_n - \hat{R}_a(\theta;q)\} + \\ + \left\| \frac{\partial \hat{R}_a}{\partial p}(\theta;x) \right\|^2 + \left\| \frac{\partial \hat{J}_a}{\partial p}(\theta;x) \right\|^2, \end{aligned} \tag{16}$$

where $c > 0$ is a constant value that is added to impose the positive definiteness of $\hat{R}_a(\theta;q)$.

Combining all these residual functions together, the final cost function to be minimized by the neural network is

$$\begin{aligned} \mathscr{L}(\theta;x,x^\star) = f_{\text{eq}}(\theta;x^\star) + f_{\text{lyap}}(\theta;x) + \\ + f_{\text{match}}(\theta;x) + f_{\text{struct}}(\theta;x). \end{aligned} \tag{17}$$

This cost function encodes the family of all admissible solutions of the IDA-PBC control design methodology. A neural IDA-PBC surrogate control input $\hat{u}$ associated to the actual u in (6) is given in the following proposition.

Proposition 1: Suppose that the hypotheses in Theorem 2.1 and Lemma 1 hold for the underactuated pH system (1) with desired equilibrium point $x^\star$ and with NN triplets $\{\hat{H}_d(\theta;x), \hat{J}_d(\theta;x), \hat{R}_d(\theta;x)\}$. Let θ^* be the minimizer of the cost function $\mathscr{L}(\theta;x,x^\star)$ in (17). Consider the pH system (1)-(2) in closed-loop with the neural IDA-PBC controller

$$\begin{aligned} \hat{u} = (g^\top g)^{-1} g \Bigg([\hat{J}_d(\theta^\star;x) - \hat{R}_d(\theta^\star;x)] \frac{\partial \hat{H}_d}{\partial x}(\theta^\star;x) \\ - [J(x) - R(x)] \frac{\partial H}{\partial x}(x) \Bigg). \end{aligned} \tag{18}$$

Then the desired equilibrium x^* can be made locally *practically* exponentially stable for a sufficiently large (wide and deep) NN $\{\hat{H}_d(\theta;x), \hat{J}_d(\theta;x), \hat{R}_d(\theta;x)\}$.

Proof: By Lemma 1, the closed-loop system will take the form of (4) perturbed additively by a nonlinear function of the approximation error $\varepsilon > 0$ and the state x. Since the desired Hamiltonian $H_d(x)$ is required to be strictly convex around $x^\star$ as formulated in $f_{\text{lyap}}(\theta^*;x)$, the function $H_d(x)$ is locally quadratic at $x^\star$. Correspondingly, the linearization of (4) around $x^\star$ becomes a linear autonomous system, which is stable by Theorem 2.1. In other words, the non-perturbed system (4) is locally exponentially stable and consequently admits a quadratic Lyapunov function. By the boundedness of $g(x)$ in the neighborhood of $x^\star$, this implies that the perturbed system is locally input-to-state stable [22] around $x^\star$ with respect to the ε as the perturbation input. Following Lemma 1, this perturbation can be made arbitrary small for sufficiently large NN so that an arbitrary small ball around $x^\star$ can be made attractive. ∎

We remark that the IDA-PBC formulation above does not impose any condition on the desired damping in the actuated coordinates. Thus, it is a free positive definite parameter that can be freely assigned to modify the closed-loop performance of the system.

IV. SIMULATION RESULTS

In this section we apply the preceding approach to design controller based on the IDA-PBC methodology in two different seminal underactuated mechanical systems: the inertia wheel pendulum and the pendulum on a cart.

A. Neural network architecture

The neural network chosen for either of the systems comprises of 5 layers (the input layer, 3 hidden layers and the output layer) as shown in Figure 1. Each hidden layer consists of 20 neurons with the activation function be given by hyperbolic tangent. For each system in the next two subsections, the parameters of the NN were initialized using the Glorot Normal distribution [23]. Additionally, the cost function was minimized using ~ 1000 points randomly sampled from a uniform distribution around the desired equilibrium. The optimization routine used consists of a combination of the ADAM [24] optimizer followed by one pass of LBFGS [25] until a predetermined convergence tolerance is achieved.

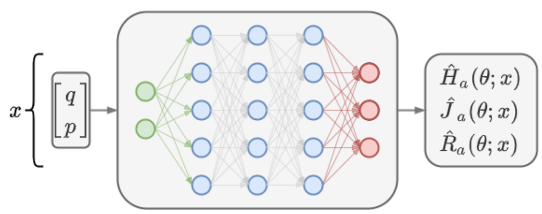

Fig. 1: Neural IDA-PBC representation. This diagram illustrates the inputs and outputs of the neural network used for solving IDA-PBC in two different underactuated systems. The generalized coordinates and momenta of the system are passed as inputs and the approximated storage, interconnection and damping functions (satisfying (5)) are obtained as outputs.

B. Inertia wheel pendulum

This mechanical system, as presented in [1, Section 5], consists of a physical pendulum with a balanced rotor at the end that produces an angular acceleration on the rotating mass which in turn generates a coupling torque at the pendulum axis (Fig. 2a).

The model that represents this system follows the description in (1) with the inertia matrix, potential function and input matrix given by $M = \begin{bmatrix} (ml^2+I) & I \\ I & I \end{bmatrix}$, $U(q) = m\overline{g}l(1+\cos(q_1))$, $B = \begin{bmatrix} 0 & 1 \end{bmatrix}^\top$, respectively, where m and l are the mass and length of the pendulum respectively, I is the inertia of the balanced rotor and $\overline{g}$ is the gravity constant.

1) Controller design: The target equilibrium corresponds to the upward position (inverted pendulum) with the inertia disk aligned $x^\star = (0,0,0,0)^\top$. The optimization method as described in Subsection IV-A explores the family of solutions in order to minimize (17). As a reminder, the only free parameter left open in the methodology presented in Section III corresponds to the desired closed-loop damping in the actuated direction. The points used during the training of the neural network were randomly sampled from a uniform distribution defined as $X \sim (x^\star - \pi/10, x^\star + \pi/10)$. The final control law is (18).

2) Numerical results: The presented results are obtained with $m = 1$, $I = 10$, $l = 1$, $\overline{g} = 9.81$ and $R_{a(2)} = 1.1$. Fig. 3 shows the time response of the generalized coordinates for different initial conditions and their corresponding (modulated) assigned interconnection matrix, (modulated) assigned damping matrix and control law over time. From these figures, we have the practical stabilization of $x^\star$ as expected from Proposition 1. Due to the approximation error, we can observe two undesirable effects. The first one is related to the non-vanishing small constant control signal after reaching the desired equilibrium (which is an unstable equilibrium of the open-loop system). The second one is related to the fact that the obtained $\hat{R}_a(q)$ has an infinitesimally negative value which violates (16). We attribute these imperfections to numerical errors in the approximation of $\frac{\partial H_d}{\partial x}(\theta; x)$ that is expected by Lemma 1.

C. Pendulum on a cart

In this mechanical system, a pendulum is attached to a movable cart, whose motion is constrained to the x-direction. A linear actuator is placed on the cart that applies a linear acceleration on the horizontal axis, which generates a coupling torque at the pendulum joint (see Fig. 2b).

The model that represents this system follows the description in (1) with the inertia matrix, potential function and input matrix be given by $M(q) = \begin{bmatrix} m_1+m_2 & m_2 l\cos(q_2) \\ m_2 l\cos(q_2) & m_2 l^2 \end{bmatrix}$, $U(q) = m_2\overline{g}l(1+\cos(q_2))$, $B = \begin{bmatrix} 1 & 0 \end{bmatrix}^\top$, respectively, where m_1 and m_2 are the mass of the cart and the mass of the pendulum respectively, l is the length of the pendulum and $\overline{g}$ is the gravity constant.

1) Controller design: In this case the target equilibrium also corresponds to the upward position (for the pendulum) and the origin for the cart, i.e. $x^\star = (0,0,0,0)^\top$. The control law is obtained in a similar way as in the inertia wheel pendulum case. The points used during the training of the neural network were also randomly sampled from a uniform distribution defined as $X \sim (x^\star - \pi/10, x^\star + \pi/10)$.

2) Numerical results: The presented results are obtained with $m_1 = 1$, $m_2 = 1$, $l = 1$, $\overline{g} = 9.81$ and $R_{a(1)} = 50.1$. Fig. 4 shows the time response of the generalized coordinates for different initial conditions and their corresponding (modulated) assigned interconnection matrix, (modulated) assigned damping matrix and control law over time. From these figures, the upright position can be stabilized as desired.

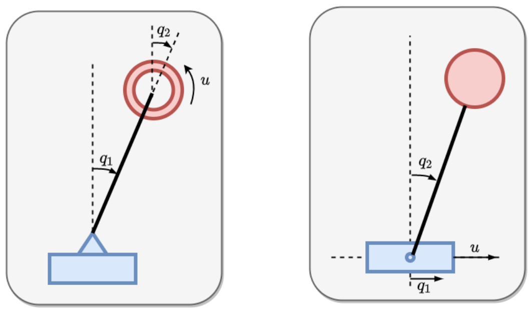

(a) Inertia wheel pendulum. (b) Pendulum on a cart.

Fig. 2: Illustrations of two underactuated mechanical systems that are used to numerically validate the Neural IDA-PBC methodology in Section IV.

V. CONCLUSIONS

In this work, we have presented a systematic approach to approximate solutions to the IDA-PBC matching equations. This methodology allows the exploration of solutions that otherwise would be too hard or even impossible to obtain analytically. It is numerically validated in two fundamental underactuated systems that have previously proven to be hard to deal with analytically [1], [3], which require intermediate steps to ease the calculations. In contrast, our technique is straightforward and enables the construction of a numerical IDA-PBC controller without requiring ansatz solutions nor apriori knowledge of the solutions.

REFERENCES

[1] Romeo Ortega, Arjan van der Schaft, Bernhard Maschke, and Gerardo Escobar. Interconnection and damping assignment passivity-based control of port-controlled Hamiltonian systems. *Automatica*, 38(4):585–596, April 2002.

[2] Fabio Gomez-Estern, Romeo Ortega, Francisco R Rubio, and Javier Aracil. Stabilization of a class of underactuated mechanical systems via total energy shaping. In *Proceedings of the 40th IEEE Conference on Decision and Control*, volume 2, pages 1137–1143. IEEE, 2001.

[3] J.A. Acosta, R. Ortega, A. Astolfi, and A.D. Mahindrakar. Interconnection and damping assignment passivity-based control of mechanical systems with underactuation degree one. *IEEE Transactions on Automatic Control*, 50(12), December 2005.

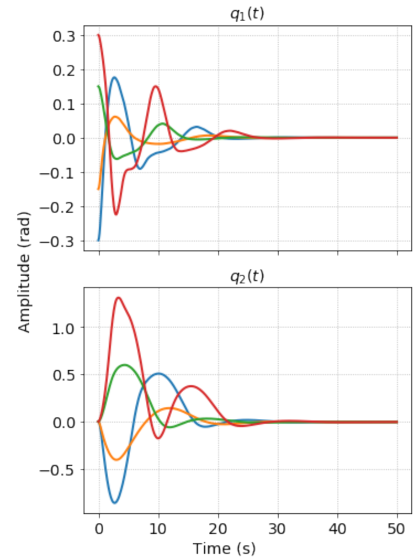

(a) Time response of the generalized coordinates for different initial conditions of q_1.

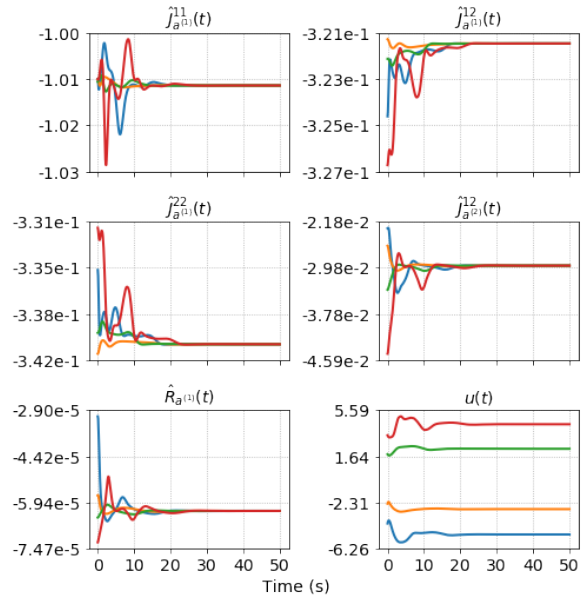

(b) Corresponding interconnection, damping and control signal values for the trajectories presented in Fig.3a.

Fig. 3: Simulation results of the Inertia wheel pendulum system. On the top, the time response of thi pendulum $q_1(t)$ and the inertia wheel $q_2(t)$ for different initial values of the underactuated coordinate. The controller based on Neural IDA-PBC is capable of stabilizing the origin in finite time. On the bottom, the corresponding values of the modulated interconnection matrix $\hat{J}_a(q)$, the modulated damping matrix $\hat{R}_a(q)$ and the control signal for the trajectories of each one of the initial conditions.

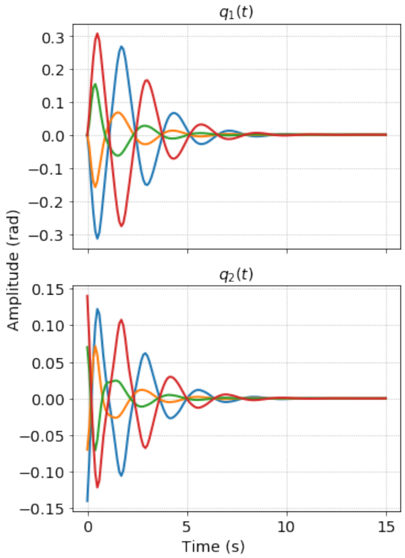

(a) Time response of the generalized coordinates for different initial conditions of q_2.

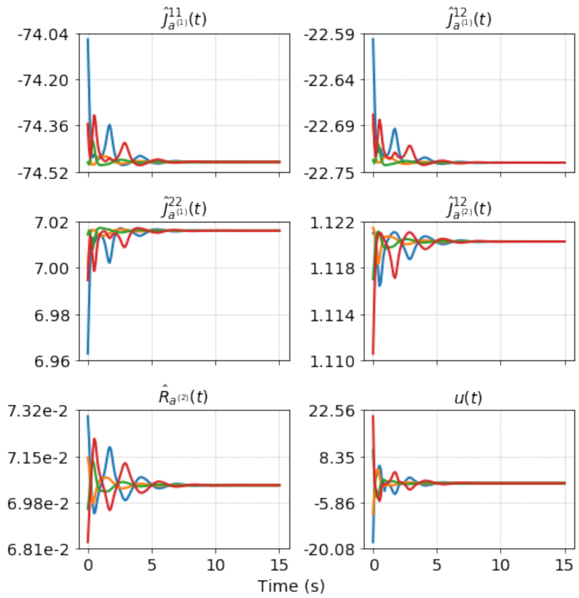

(b) Corresponding interconnection, damping and control signal values for the trajectories presented in Fig.4a.

Fig. 4: Simulation results of the pendulum on a cart system. On the top, the time response of the pendulum $q_1(t)$ and the inertia wheel $q_2(t)$ for different initial values of the underactuated coordinate. The controller based on Neural IDA-PBC is capable of stabilizing the origin in finite time. On the bottom, the corresponding values of the modulated interconnection matrix $\hat{J}_a(q)$, the modulated damping matrix $\hat{R}_a(q)$ and the control signal for the trajectories of each one of the initial conditions.

[4] Isaac Gandarilla, Víctor Santibáñez, Jesús Sandoval, and Ricardo Campa. Joint position regulation of a class of underactuated mechanical systems affected by LuGre dynamic friction via the IDA-PBC method. *International Journal of Control*, pages 1–13, 2020.

[5] Mutaz Ryalat and Dina Shona Laila. IDA-PBC for a class of underactuated mechanical systems with application to a rotary inverted pendulum. In *In Proc. 52nd IEEE Conference on Decision and Control*, pages 5240–5245, 2013.

[6] Pierluigi Arpenti, Fabio Ruggiero, and Vincenzo Lippiello. A constructive methodology for the IDA-PBC of underactuated 2-dof mechanical systems with explicit solution of PDEs. *International Journal of Control, Automation and Systems*, 20(1):283–297, 2022.

[7] Alejandro Donaire, Jose Guadalupe Romero, Romeo Ortega, Bruno Siciliano, and Martin Crespo. Robust IDA-PBC for underactuated mechanical systems subject to matched disturbances. *International Journal of Robust and Nonlinear Control*, 27(6):1000–1016, 2017.

[8] Christopher I. Byrnes, Francesco Delli Priscoli, and Alberto Isidori. *Output regulation of uncertain nonlinear systems*. Birkhäuser, Boston, 1997.

[9] Alessandro Astolfi and Romeo Ortega. Immersion and invariance: a new tool for stabilization and adaptive control of nonlinear systems. *IEEE Transactions on Automatic Control*, 48(4):590–606, 2003.

[10] George Em Karniadakis, Ioannis G. Kevrekidis, Lu Lu, Paris Perdikaris, Sifan Wang, and Liu Yang. Physics-informed machine learning. *Nat Rev Phys*, 3(6):422–440, June 2021.

[11] Jin Wang, Jie Huang, and SST Yau. Approximate nonlinear output regulation based on the universal approximation theorem. *International Journal of Robust and Nonlinear Control*, 10:439–456, 04 2000.

[12] Spencer M. Richards, Felix Berkenkamp, and Andreas Krause. The Lyapunov Neural Network: Adaptive Stability Certification for Safe Learning of Dynamical Systems. *arXiv:1808.00924*, October 2018.

[13] Lars Grüne. Computing Lyapunov functions using deep neural networks. *arXiv:2005.08965*, November 2020.

[14] Ya-Chien Chang, Nima Roohi, and Sicun Gao. Neural Lyapunov Control. *arXiv:2005.00611*, December 2020.

[15] Ya-Chien Chang and Sicun Gao. Stabilizing Neural Control Using Self-Learned Almost Lyapunov Critics. *arXiv:2107.04989*, July 2021.

[16] Liang Xu, Muhammad Zakwan, and Giancarlo Ferrari-Trecate. Neural Energy Casimir Control. *arXiv:2112.03339*, December 2021.

[17] Santiago Sanchez-Escalonilla, Rodolfo Reyes-Baez, and Bayu Jayawardhana. Total Energy Shaping with Neural Interconnection and Damping Assignment – Passivity Based Control. *Accepted in 4th Annual Learning for Dynamics and Control Conference*, July 2022.

[18] Kurt Hornik, Maxwell Stinchcombe, and Halbert White. Multilayer feedforward networks are universal approximators. *Neural Networks*, 2(5):359–366, January 1989.

[19] Arjan van der Schaft and Dimitri Jeltsema. Port-Hamiltonian systems theory: An introductory overview. *Foundations and Trends in Systems and Control*, 1(2-3):173–378, 2014.

[20] Arjan van der Schaft. *L2-Gain and Passivity Techniques in Nonlinear Control*. Springer International Publishing, 2017.

[21] G. Cybenko. Approximation by superpositions of a sigmoidal function. *Mathematics of Control, Signals, and Systems*, 2(4):303–314, December 1989.

[22] Hassan K. Khalil. *Nonlinear control*. Pearson, Boston, 2015.

[23] Xavier Glorot and Yoshua Bengio. Understanding the difficulty of training deep feedforward neural networks. In *Proc. of the 13th International Conference on Artificial Intelligence and Statistics*, pages 249–256, March 2010.

[24] Diederik P. Kingma and Jimmy Ba. Adam: A Method for Stochastic Optimization. *arXiv:1412.6980*, January 2017.

[25] Dong C. Liu and Jorge Nocedal. On the limited memory BFGS method for large scale optimization. *Mathematical Programming*, 45(1):503–528, August 1989.